Grid-connected of photovoltaic module using nonlinear control

El Fadil, H.; Giri, F.; Guerrero, Josep M.

Published in:
3rd IEEE International Symposium on Power Electronics for Distributed Generation Systems (PEDG) 2012

DOI (link to publication from Publisher):
10.1109/PEDG.2012.6253989

Publication date:
2012

Document Version
Early version, also known as pre-print

This document is a preprint of the paper: Fadil, H.E.; Giri, F.; Guerrero, J.M.; , "Grid-connected of photovoltaic module using nonlinear control," Power Electronics for Distributed Generation Systems (PEDG), 2012 3rd IEEE International Symposium on , vol., no., pp.119-124, 25-28 June 2012.
doi: 10.1109/PEDG.2012.6253989
URL: http://ieeexplore.ieee.org/stamp/stamp.jsp?tp=&arnumber=6253989&isnumber=6253967

Grid-Connected of Photovoltaic Module Using Nonlinear Control

H. El Fadil, F. Giri, Josep M. Guerrero

***Abstract*—The problem of controlling single-phase grid connected photovoltaic (PV) system is considered. The control objective is fourfold: (i) asymptotic stability of the closed loop system, (ii) maximum power point tracking (MPPT) of PV module (iii) tight regulation of the DC bus voltage, and (iv) unity power factor (PF) in the grid. A nonlinear controller is developed using the backstepping design technique based on an averaged nonlinear model of the whole controlled system. The model accounts, on the one hand, for the nonlinear dynamics of the underlying boost converter and inverter and, on the other, for the nonlinear characteristic of PV panel. It is formally shown, through theoretical analysis and simulation results, that the proposed controller does achieve its objectives.**

I. Introduction

With the deregulation of electricity markets and thrust to reduce greenhouse gas emissions from the traditional electric power generation systems, renewable energy resources such as wind turbines, photovoltaic panels, gas turbines and fuel cells, has gained a significant opportunity as new means of power generation to meet the growing demand for electric energy. Solar energy is considered to be one of the most useful natural energy sources because it is free, abundant, pollution-free, and most widely distributed. It can be used either at remote regions as standalone apparatus or in urban applications as grid interactive power source [1]. On the other hand, a significant technology progress has been achieved over the few past years increasing efficiency of solar cells. The rapid growth of solar industry has expanded the importance of PV systems making them more reliable and efficient, especially for utility power in distributed generation (DG) (see Fig. 1) at medium and low voltages power systems. Implementing distributed energy resources (DER), into interconnected grids could be part of the solution to meet the rising electricity demand ([2], [3]). DG technologies are currently being improved through several research projects toward the development of smart grids.

PV energy applications are divided into two categories: stand-alone systems and grid-connected systems. Stand-alone systems require a battery bank to store the PV energy; this is suitable for low-power systems. On the other hand, grid-connected PV systems do not require battery banks; they are resorted generally in high power applications. The main purpose of the grid-connected system is to extract the maximal quantity possible of solar array energy and restitute it to grid with a unity power factor, despite changing atmospheric conditions (temperature and radiation).

PV grid-connected systems represent the most important field applications of solar energy ([4], [5], [6]). In general, a photovoltaic grid-connected system can be seen as a two-stage grid-connected inverter (Fig.1). The first stage is a dc-dc converter controlled so that the photovoltaic system operates in optimal condition i.e. seeking maximum power point tracking (MPPT). The second stage is a dc-ac converter that controlled in a way that allows a grid connection with a unity power factor (PF). To this end, the output current (entering the grid) must be sinusoidal and in phase with the grid voltage. The dc-dc and dc-ac converters operate independently making easier the whole system control.

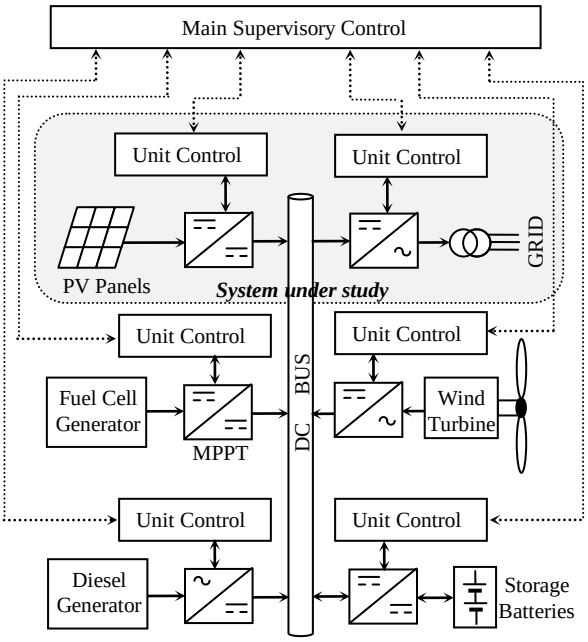

Fig.1: Control architecture in distributed energy resources

The present paper is focusing on the problem of controlling single phase grid-connected PV power generation systems (Fig. 1). The control objective is fourfold: (i) global asymptotic stability of the whole closed-loop control system; (ii) achievement of MPPT of the PV array; (iii) ensuring a grid connection with unity PF; and (iv) ensuring a tight regulation of the dc-bus voltage. These objectives must be met despite changes of the climatic variables (temperature and radiation).

Manuscript received October, 2011.

H. El Fadil is with the National School of Applied Sciences (ENSA), Ibn Tofail University, Kénitra, Morocco (corresponding author; e-mails: el_fadil_hassan@univ-ibntofail.ac.ma)

F. Giri is with the GREYC Lab, UMR CNRS, University of Caen, 14032, Caen, France (giri@greyc.ensicaen.fr).

J.M. Guerrero is with the Aalborg university, Denmark, (e-mail: josep.m.guerrero@upc.edu, joz@et.aau.dk).

To this end, a nonlinear controller is developed using the backstepping design technique based on large-signal nonlinear model of the whole system. A theoretical analysis is developed to show that the controller actually meets its objectives a fact that is confirmed by simulation.

The paper is organized as follows: the single phase grid connected PV system is described and modeled in Section II. Section III is devoted to controller design and analysis. The controller tracking performances are illustrated by numerical simulation in Section IV.

II. Presentation and Modeling of Grid Connected PV System

A typical configuration of a single-phase grid connected photovoltaic system is shown in Fig. 2. It consists of a solar array, an input capacitor C_i, a boost dc-dc converter which is used for boosting the array voltage and achieving MPPT for PV array, a DC link capacitor C_{dc}, a single-phase full-bridge inverter (including four power semiconductors) that is based upon to ensure a DC-AC power conversion a unity PF, a filter inductor L_g, and an isolation transformer.

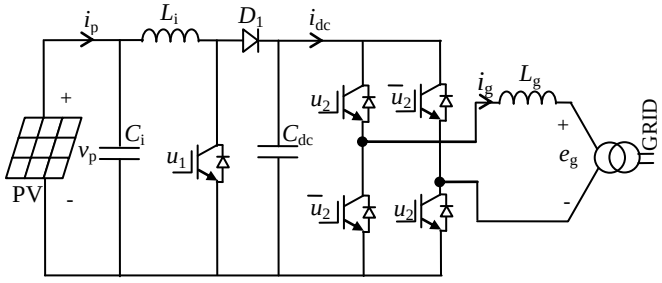

Fig.2: Single phase grid connected PV system

A. PV array model

Typical ($I_p - V_p$) characteristics of solar cells arranged in N_p-parallel and N_s-series are analytically defined by the following standard equation:

$$I_p = N_p I_{ph} - N_p I_o \left\{ \exp\left[A\left(V_p + \frac{N_s I_p R_s}{N_p} \right) \right] - 1 \right\} - \frac{N_p}{R_{sh}} \left(\frac{V_p}{N_s} + \frac{I_p R_s}{N_p} \right) \qquad (1)$$

The meaning and typical values of the parameters in (1) can be found in many places (see e.g. [7], [8], [12]). To fix idea, the PV array module considered in this paper is the NU-183E1. The corresponding electrical characteristics are listed in Table I. The associated power-voltage (P-V) characteristics under changing climatic conditions (temperature and radiation) are shown in Figs. 3 and 4. These emphasize the maximum power points (MPP) M1 to M4, the coordinates of which are shown in Table II. The data in Table I and Table II will be used latter for simulation purpose.

TABLE I: ELECTRICAL SPECIFICATIONS FOR THE SOLAR MODULE NU-183E1

Parameter	Symbol	Value
Maximum Power,	P_m	183.1W
Short circuit current	I_{scr}	8.48 A
Open circuit voltage	V_{oc}	30.1V
Maximum power voltage	V_m	23.9 V
Maximum power current	I_m	7.66A
Number of parallel modules	N_p	1
Number of series modules	N_s	48

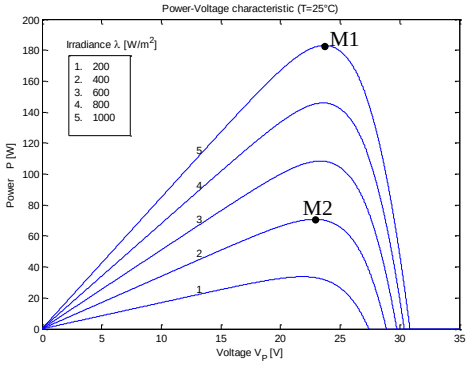

Fig.3: (*P-V*) characteristics of The PV module NU-183E1 with constant temperature and varying radiation

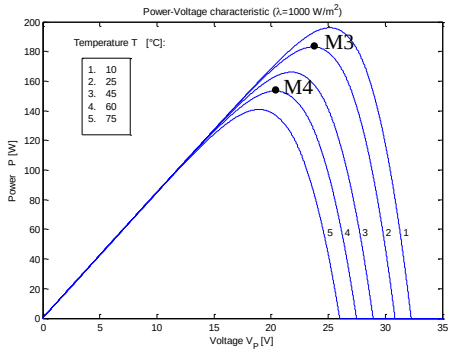

Fig.4: (*P-V*) characteristics of The PV module NU-183E1 with constant radiation and varying temperature

TABLE II: MAXIMUM POWER POINTS (MPP) IN FIG.3 AND FIG.4

MPP	V_m	P_m
M1	23.82 V	183.1 W
M2	22.94 V	70.8 W
M3	23.82 V	183.1 W
M4	20.38 V	153.4 W

B. Overall system model

The control input u_1 and u_2 of the boost converter and for the inverter, respectively, are a PWM signals taking values in the set $\{0,1\}$. Applying the Kirchoff's laws, successively with $u_1 = 1$ and $u_1 = 0$, to the boost converter circuit and with $u_2 = 1$ and $u_2 = 0$, to the inverter circuit of of Fig. 2 one obtains the following averaged model [9]:

$$\frac{dx_1}{dt} = \frac{1}{C_i}(\bar{i}_p - x_2) \tag{2a}$$

$$\frac{dx_2}{dt} = -(1-\mu_1)\frac{x_3}{L_i} - \frac{R_i}{L_i}x_2 + \frac{x_1}{L_i} \tag{2b}$$

$$\frac{dx_3}{dt} = (1-\mu_1)\frac{x_2}{C_{dc}} - (2\mu_2 - 1)\frac{x_4}{C_{dc}} \tag{2c}$$

$$\frac{dx_4}{dt} = (2\mu_2 - 1)\frac{x_3}{L_g} - \frac{R_g}{L_g}x_4 - \frac{e_g}{L_g} \tag{2d}$$

where R_i is the equivalent series resistance (ESR) of input inductance L_i.

and where x_1, x_2, x_3, x_4, $\bar{i}_p$, μ_1 and μ_2 denote the average values of the system variable (Table III). All variables averaging are performed over switching periods. Consequently, the quantities μ_1 and μ_2, commonly called duty ratios, vary continuously in the interval [0 1] and act as the input control signals.

TABLE III: MODEL VARIABLE AVERAGING

Physical variable	Its Averaged Version
PV voltage v_p	x_1
inductor current i_{Li}	x_2
dc bus voltage v_{dc}	x_3
grid current i_{Lg}	x_4
PV current i_p	$\bar{i}_p$
boost converter binary control input u_1	μ_1
inverter binary control input u_2	μ_2

III. CONTROLLER DESIGN

In this section, we aim at designing a controller that will be able to ensure: (i) a global stability of closed loop system, (ii) a perfect MPPT (whatever the position of the PV panel). Specifically, the controller must enforce the voltage x_1 to track, as accurately as possible, the unknown (and slowly varying) voltage V_m. Note that V_m is unknown because it depends on the temperature T and solar variation λ and these are not supposed to be measured; (iii) a unity PF in the grid; and (iv) a tight regulation of the dc bus voltage x_3.

A. Controlling the boost converter to meet MPPT

Recall that the control objective is to enforce the voltage x_1 to track the optimal point V_m. To this end, the backstepping design principles are invoked [10].

Design Step 1. Let us introduce the following tracking error:

$$z_1 = x_1 - V_m \tag{3}$$

Achieving the tracking objective amounts to enforcing the error z_1 to vanish. To this end, the dynamics of z_1 have to be clearly defined. Deriving (3), it follows from (2a) that

$$\dot{z}_1 = \frac{1}{C_i}(\bar{i}_p - x_2) - \dot{V}_m \tag{4}$$

In the above equation, the quantity x_2/C_i stands as a virtual control variable. Let us consider the following Lyapunov function

$$V_1 = 0.5z_1^2 \tag{5}$$

The time-derivative of V_1 along the trajectory of (4) is

$$\dot{V}_1 = z_1\left(\frac{-x_2}{C_i} + \frac{\bar{i}_p}{C_i} - \dot{V}_m\right) \tag{6}$$

Equation (6) shows that the tracking error z_1 can be regulated to zero if $x_2/C_i = \alpha_1$ where α_1 is a stabilizing function defined by

$$\alpha_1 = \frac{i_p}{C_i} + c_1 z_1 - \dot{V}_m \tag{7}$$

where $c_1 > 0$ is a design parameter. Since x_2/C_i is not the actual control input, one can only seek the convergence of the error $x_2/C_i - \alpha_1$ to zero. We then define the following second error variable:

$$z_2 = x_2/C_i - \alpha_1 \tag{8}$$

The next step is to determine a variation law for control signal μ_1 so that the set of errors z_1 and z_2 vanish asymptotically. But, let us first establish some useful equations. Equation (4) becomes, using (8)

$$\dot{z}_1 = -c_1 z_1 - z_2 \tag{9}$$

Also, the derivative (6) of the Lyapunov function is rewritten

$$\dot{V}_1 = -c_1 z_1^2 - z_1 z_2 \tag{10}$$

Design Step 2. The objective now is to enforce the error variables (z_1, z_2) to vanish. To this end, let us first determine the dynamics of z_2. Deriving (8) and using (2b), and (9), one obtains

$$\dot{z}_2 = -(1-\mu_1)\frac{x_3}{L_i C_i} - \frac{R_i}{L_i C_i}x_2 + \frac{x_1}{L_i C_i} - \frac{1}{C_i}\frac{d\bar{i}_p}{dt} + c_1^2 z_1 + c_1 z_2 + \ddot{V}_m \tag{11}$$

We are finally in a position to make a convenient choice of the control signal μ_1 to stabilize the whole system with state vector is (z_1, z_2). Consider the augmented Lyapunov function candidate

$$V = V_1 + 0.5z_2^2 = 0.5z_1^2 + 0.5z_2^2 \tag{12}$$

Our goal is to make $\dot{V}$ non-positive definite

$$\dot{V} = \dot{V}_1 + z_2\dot{z}_2 = -c_1 z_1^2 - c_2 z_2^2 + z_2\left[-z_1 + c_2 z_2 + \dot{z}_2\right] \tag{13}$$

where $c_2 > 0$ is a design parameter. Equation (13) shows that the equilibrium (z_1, z_2)=(0,0) is globally asymptotically stable if

$$\dot{z}_2 = -c_2 z_2 + z_1 \tag{14}$$

Combining (11) and (14) one gets the following control law

$$\mu_1 = 1 - \frac{1}{x_3}\left\{L_i C_i\left[(c_1^2 - 1)z_1 + (c_1 + c_2)z_2 + \ddot{V}_m\right] + x_1 - R_i x_2 - L_i \dot{\hat{i}}_p\right\} \tag{15}$$

B. Generation of the optimal voltage V_m

The MPP (V_m, P_m) is reached when:

$$\left.\frac{\partial P}{\partial v_p}\right|_{v_p = V_m} = 0 \tag{16}$$

with $P = v_p i_p$ being the PV power. That is, the controller must keep dP/dv_p equals zero, whatever the radiation λ and the temperature T, by acting on the duty cycle μ_1. Then, the optimal voltage V_m can be generated using a PI regulator as shown in Fig. 5. This regulator (denoted PI-1 in Fig. 5) is defined as follows:

$$V_m = G_1(s)\varepsilon_p \tag{17a}$$

where

$$G_1(s) = k_1 \frac{(1 + \tau_1 s)}{\tau_1 s} \tag{17b}$$

$$\varepsilon_p = \frac{dP}{dv_p} \tag{17c}$$

where s denotes the Laplace variable.

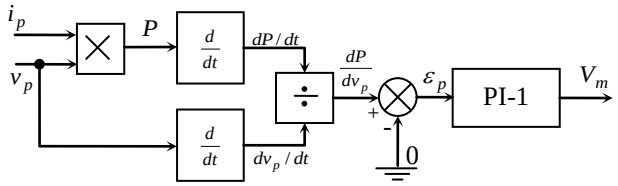

Fig.5: Optimal voltage generation diagram

C. Controlling the inverter to meet unity PF in the grid and regulation of the dc bus voltage objectives

1) Unity PF objective

The unity PF objective means that the grid current i_{Lg} should be sinusoidal and in phase with the AC grid voltage e_g. We therefore seek a regulator that enforces the current x_4 to tack a reference signal x_4^* of the form:

$$x_4^* = \beta e_g \tag{18}$$

At this point β is any real positive parameter that is allowed to be time-varying. The regulator will now be designed using the backstepping technique [10]. Let us introduce the following current error:

$$z_3 = x_4 - x_4^* \tag{19}$$

In view of (2d), the above error undergoes the following dynamics:

$$\dot{z}_3 = \dot{x}_4 - \dot{x}_4^* = (2\mu_2 - 1)\frac{x_3}{L_g} - \frac{R_g}{L_g}x_4 - \frac{e_g}{L_g} - \dot{x}_4^* \tag{20}$$

To get a stabilizing control law for this first-order system, consider the quadratic Lyapunov function:

$$V_3 = 0.5 z_3^2 \tag{21}$$

It can be easily checked that the time-derivative $\dot{V}_3$ is a negative definite function of z_3 if the control input μ_2 is chosen to be:

$$\mu_2 = \frac{1}{2} + \frac{1}{2x_3}\left\{R_g x_4 + e_g + L_g\left(-c_3 z_3 + \dot{x}_4^*\right)\right\} \tag{22}$$

where $c_3 > 0$ is a design parameter. Indeed, with this choice one has

$$\dot{z}_3 = -c_3 z_3 \tag{23}$$

$$\dot{V}_3 = -c_3 z_3^2 \tag{24}$$

This means, in particular, that the equilibrium $(z_3 = 0)$ is globally asymptotically stable and therefore the unity PF is asymptotically achieved.

2) DC bus voltage regulation objective

Now, the aim is to design a variation law for the ratio β in (18) so that the inverter dc input voltage $x_3 =< v_{dc} >$ is steered to a given constant reference $V_d > 0$. To this end, the following PI control law (called PI-2) is used:

$$\beta = G_2(s)\varepsilon_{dc} \tag{25a}$$

where

$$G_2(s) = k_2 \frac{(1 + \tau_2 s)}{\tau_2 s} \tag{25b}$$

$$\varepsilon_{dc} = x_3 - V_d \tag{25c}$$

The performances of the controller, consisting of the control laws (25a-c), (22) and (15) are described in the following theorem.

Theorem 1 (*main result*). Consider the single-phase grid-connected PV system shown in Fig. 2, represented by its average model (2a-d), together with the controller consisting of the control laws (15), (22) and (25a-c). Then, one has the following results:

i) The closed loop system is globally asymptotically stable.

ii) The tracking error $z_1 = x_1 - V_m$ vanishes exponentially, implying MPPT achievement (because V_m is the optimal PV voltage corresponding to maximum power i.e. $dP/dv_p = 0$). Interestingly, V_m is computed online according to the law (18a-c).

iii) The error $z_3 = x_4 - x_4^*$ converges to zero ensuring a unity PF (because $x_4^* = \beta e_g$).

iv) The tracking error $\varepsilon_{dc} = x_3 - V_d$ converges to zero guaranteeing a tight regulation of the dc bus voltage.

IV. Simulation Results

The theoretical performances, described by Theorem 1, of the proposed nonlinear controller are now illustrated by simulation. The experimental setup, described by Fig. 6, is simulated using MATLAB. The characteristics of the controlled system are listed in Table IV. Let us emphasize that the controlled system is simulated using its instantaneous model. The averaged model (2a-d) is in effect used only in controller design. The control design parameters are given values of Table V which proved to be convenient. The resulting closed-loop control performances are illustrated by Fig 7 to Fig 10.

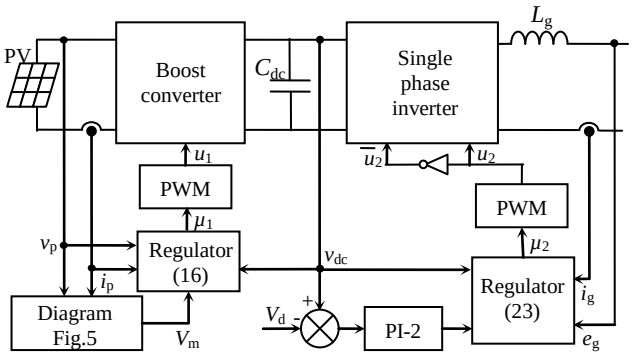

Fig.6: Experimental bench for single phase grid connected system control

TABLE IV: CHARACTERISTICS OF CONTROLLED SYSTEM

Parameter	Symbol	Value
PV array	PV power	183.1W
	PV model	NU-183E1
Boost converter	C_i	4700µF
	L_i	1mH
	R_i	0.65Ω
DC link capacitor	C_{dc}	6800µF
Grid filter inductor	L_g	2.2mH
	R_g	0.47 Ω
PWM	Switching frequency	25kHz
Grid	Transformer ratio	22:220
	AC source	220V
	Line frequency	50Hz

TABLE V: CONTROLLER PARAMETERS

Parameter	Symbol	Value
Design parameters	c_1	10^5
	c_2	10^4
	c_3	10^4
PI regulator (PI-1)	k_1	0.5
	τ_1	10ms
PI regulator (PI-2)	k_2	0.02
	τ_2	30ms
Desired DC bus voltage	V_d	48V

A. *Radiation change effect*

Fig. 7 illustrates the perfect MPPT in presence of radiation changes. Specifically, the radiation varies between 400 W/m^2 and 1000 W/m^2, meanwhile the temperature is kept constant, equal to 298.15K (i.e. 25°C). The figure shows that the captured PV power varies between 70.8 W and 183.1 W. These values correspond (see Fig. 3) to the maximum points (M2 and M1) of the curves associated to the considered radiations, respectively. The figure, also shows that the DC bus voltage v_{dc} is regulated to its desired value V_d=48V. Fig. 8 illustrates the grid current i_{Lg} and the grid voltage e_g. This figure clearly shows that the current i_{Lg} is sinusoidal and in phase with the voltage e_g, proving unity PF achievement.

B. *Temperature variation effect*

Fig. 9 illustrates the controller behavior when facing temperature changes. Specifically, the temperature T varies between 298.15K and 333.15 K (i.e. between 25°C and 60°C), while the radiation λ is constant equal to 1000 W/m^2. It is seen that the controller keeps the whole system at the optimal operation conditions. Indeed, the captured PV power P achieves the values 183.1W or 153.4W corresponding (on the power curves of Fig. 4) to the maximum points (M3 and M4) associated to the temperatures 333.15K and 298.15K, respectively. The figure also shows that the DC bus voltage v_{dc} is regulated to its desired value V_d=48V. Fig. 10 illustrates the grid current i_{Lg} and the grid voltage e_g. This figure also shows that the current i_{Lg} is sinusoidal and in phase with the voltage e_g, which proves the unity PF achievement.

V. Conclusion

The problem of controlling a single-phase grid connected PV system has been considered. The controller is obtained from the nonlinear average model (3) using nonlinear control technique. Using both a theoretical analysis and simulation, it is proved that the controller does meet the performances for which it was designed, namely:

(i) global asymptotic stability of the closed-loop system,
(ii) perfect maximum power point tracking of PV array,
(iii) good unity power factor in the grid,
(iv) tight regulation of the DC bus voltage.

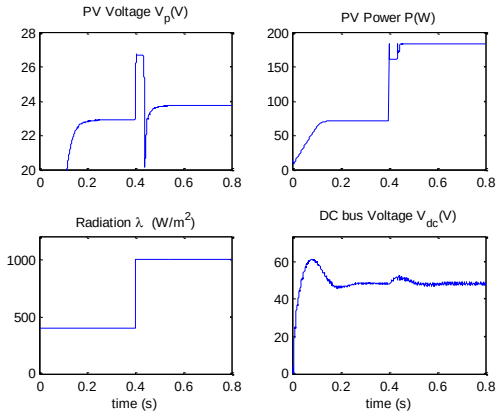

Fig.7 : MPPT and DC bus voltage behavior in presence of radiation changes.

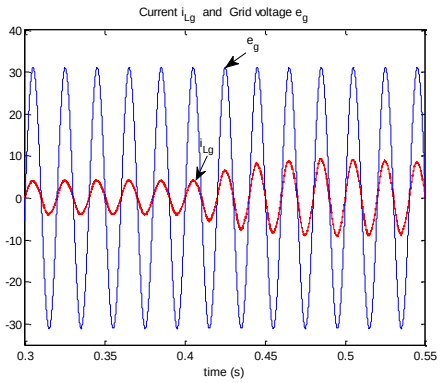

Fig.8 : Unity PF behavior in presence of radiation changes

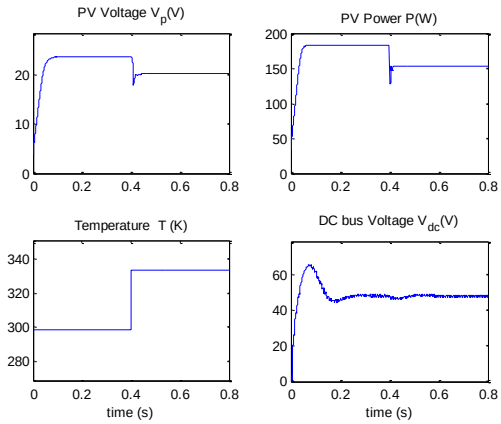

Fig.9 : MPPT and DC bus voltage behavior in presence of temperature changes.

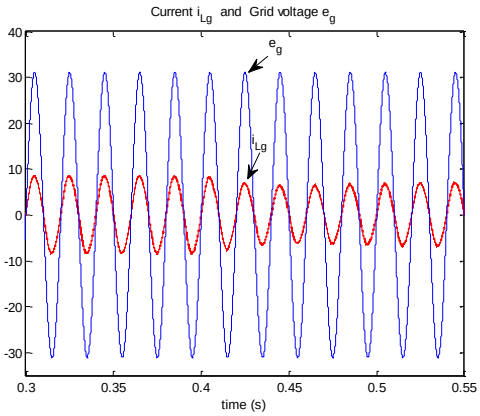

Fig.10 : Unity PF behavior in presence of temperature changes

REFERENCES

[1] Shimizu T, Hashimoto O, Kimura G. A novel high-performance utilityinteractive photovoltaic inverter system. *IEEE Trans Power Electron* 2003;18:704–11.

[2] Ortjohann E., Lingemann M., Mohd A., Sinsukthavorn W., Schmelter A., Hamsic N. and Morton, D.. A General Architecture for Modular Smart Inverters, *IEEE ISIE*, Cambridge, England, 2008.

[3] Akorede M.F., H. Hizam, E. Pouresmail. Distributed energy resources and benefits to environment. *Renewable and Sustainable Energy reviews*, 14, pp. 724-734, 2010.

[4] Wu Libo, Zhao Zhengming, Liu Jianzheng , "A single-stage three-phase grid-connected photovoltaic system with modified MPPT method and reactive power compensation" *IEEE Transactions on Energy Conversion*, v 22, n4, pp. 881-886, December, 2007.

[5] Abeyasekera T, Johnson CM, Atkinson D, Amstrong M. Suppression of line voltage related distortion in current controlled grid connected inverters. IEEE Trans Power Electron;20:1393–401, 2005.

[6] Barbosa PG, Braga HAC, Barbosa MC, Teixeria EC. Boost current multilevel inverter and its application on single phase grid connected photovoltaic system. IEEE Trans Power Electron;21:1116–24, 2006.

[7] Enrique J.M., E. Duran, M. Sidrach-de-Cardona, J.M. Andujar. "Theoritical assessment of the maximum power point tracking efficiency of photovoltaic facilities with different converter topologies". *Solar Energy*, 81, pp. 31-38, 2007.

[8] Chen-Chi Chu, Chieh-Li Chen. "Robust maximum power point tracking method for photovoltaic cells: A sliding mode control approach". *Solar Energy*, 83, pp. 1370–1378, 2009.

[9] Krein P.T., Bentsman, J., Bass, R. M., & Lesieutre, B. "On the use of averaging for analysis of power electronic system". *IEEE Transactions on Power Electronics*, 5(2), pp. 182–190, 1990.

[10] Krstić M., I. Kanellakopoulos and P. V. Kokotović. "Nonlinear and adaptive control design". John Willy & Sons, NY, 1995.

[11] Mastromauro, R.A. Liserre, M. Kerekes, T. Dell'Aquila, A. "A Single-Phase Voltage-Controlled Grid-Connected Photovoltaic System With Power Quality Conditioner Functionality". *IEEE Transactions on Indust. Electronics*, 56(11), pp. 4436–4444, 2009.

[12] El Fadil, H. and Giri, F. "Climatic sensorless maximum power point tracking in PV generation systems". *Control Engineering Practice* (ELSEVIER), Vol. 19, N.5, pp. 513–521, May 2011